



GENE B13-02080-00-03NP

TECHNICAL SERVICES
GE Nuclear Energy
175 Curtner Avenue, San Jose, CA 95125

GE-NE-B13-02080-00-03NP
DRF #B13-02080-00-03
Class I
August 2000

THE EVALUATION OF LIMERICK UNIT 2 SHROUD H4 CRACKING FOR TWO FUEL CYCLES OF OPERATION

August 2000

Prepared for

Limerick Unit 2

Prepared by

GE Nuclear Energy
175 Curtner Avenue
San Jose, CA 95125



THE EVALUATION OF LIMERICK UNIT 2
SHROUD H4 CRACKING
FOR TWO FUEL CYCLES OF OPERATION

August 2000

Prepared by: *Randy Stark*
R. R. Stark, Senior Engineer
Structural Assessment & Mitigation

R M Horn
R. M. Horn, Engineering Fellow
Structural Assessment & Mitigation

Verified by: *S Ranganath*
S. Ranganath, Engineering Fellow
Structural Assessment & Mitigation

Approved by: *T A Caine*
for T. A. Caine, Manager
Structural Assessment & Mitigation



DISCLAIMER OF RESPONSIBILITY
Important Notice Regarding the Contents of this Report
Please Read Carefully

The only undertaking of General Electric Company respecting information in this document are contained in the contract between PECO and General Electric Company, and nothing contained in this document shall be construed as changing the contract. The use of this information by anyone other than PECO or for any purpose other than that for which it is intended is not authorized; and with respect to any unauthorized use, General Electric Company makes no representation or warranty, and assumes no liability as to the completeness, accuracy, or usefulness of the information contained in this document.



Table of Contents

<u>Subject</u>	<u>Page No.</u>
1. EXECUTIVE SUMMARY.....	4
2. BACKGROUND AND SUMMARY OF H4 CRACK INDICATIONS.....	5
3. STRUCTURAL MARGIN ASSESSMENT.....	6
3.1. ASSUMPTIONS	6
3.2. STRUCTURAL EVALUATION METHODOLOGY	6
3.3. H4 ANALYSIS.....	7
3.3.1. LEFM Analysis	7
3.3.2. Limit Load Analysis.....	8
3.4. ANALYSIS RESULTS	10
4. CONCLUSIONS.....	11
5. REFERENCES.....	12
<i>APPENDIX A: UT DATA.....</i>	<i>A-1</i>
<i>APPENDIX B: The Beneficial Effect of Reduced Corrosion Potential on the Stress Corrosion Crack Growth Rates of Irradiated Stainless Steel.....</i>	<i>B-1</i>
<i>APPENDIX C: Crack Growth Rates in the High Fluence H4 Shroud Weld During Operation With NobleChem™ And Hydrogen Water Chemistry</i>	<i>C-1</i>
1. Introduction	C-2
2. Factors of Improvement Observed in Laboratory Crack Growth Tests on Irradiated Materials	C-2
3. Overview of the GE Irradiated PLEDGE Model	C-3
4. Validation of the Beneficial Effects of low corrosion potential using the Irradiated PLEDGE Model.....	C-5
5. Crack Growth Rate for H4 during Operation with NobleChem™ and HWC.....	C-6
6. References	C-7



1. EXECUTIVE SUMMARY

Indications were found in the H4 weld as a result of UT inspections performed on the shroud circumferential welds at Limerick Unit 2 during the Spring 1999 RFO5 outage. The inspection data for the H4 weld is included in the Appendix A. Limerick Unit 2 has operated under normal water chemistry (NWC) for the current cycle. NobleChem™ will be implemented during the Spring 2001 RF06 outage, and the plant will be operating with Hydrogen Water Chemistry (HWC) during the following cycle. This report provides an evaluation of the structural margin for the H4 weld in the Limerick Unit 2 core shroud for two cycles of operation (the current cycle under NWC and the coming cycle under HWC with NobleChem™). The crack growth rates that are used in this updated evaluation include one cycle with NWC crack growth rate (5×10^{-5} in/hr) and reduced crack growth rate taking credit for operation during the upcoming cycle on hydrogen water chemistry with NobleChem™.

The justification for the reduced rate under NobleChem™ is based on extensive test data validating the benefit of reduced Electrochemical Corrosion Potential (ECP) during HWC and also the results of the GE Irradiated PLEDGE model which is based on fundamental principles and benchmarked by comparison with test data. Appendix B entitled "The Beneficial Effect of Reduced Corrosion Potential on the Stress Corrosion Crack Growth Rates of Irradiated Stainless Steel," describes the state-of-the art data on irradiated stainless steel and quantifies the factor of improvement resulting from reduced ECP operation. Appendix C entitled "Crack Growth Rates in the High Fluence H4 Shroud Weld During Operation with NobleChem™ and Hydrogen Water Chemistry" Describes the determination of irradiated crack growth rates based on the GE Irradiated PLEDGE model. Both studies suggest that the factor of improvement is well in excess of 10. Based on these Appendices a conservative value of 1×10^{-5} in/hr was proposed for the evaluation of the H4 weld under HWC operation. Assuming that HWC availability is 90%, (i.e. HWC operation for 90% of the time and NWC for 10% of the time), the effective crack growth rate for the coming cycle was determined to be 1.4×10^{-5} in/hr.



A structural evaluation of the H4 weld indications was performed. The initial indication was assumed to be a fully circumferential 360° crack with a depth equal to the maximum observed depth (0.11 inch) This was increased to account for UT uncertainty (0.131 in) and crack growth (5×10^{-5} in/hr x 16,000 hrs for the current cycle + 1.4×10^{-5} in/hr x 16,000 hrs for the upcoming cycle) resulting in the end-of-cycle crack depth of 1.265 in.

The allowable depth considering both the LEFM and limit load evaluations was determined to be 1.66 inch. This includes the NRC approved safety factors required in BWRVIP-01. Even with the conservative crack growth assessment, the predicted depth at the end of the next cycle will still be within the allowable value. The evaluation determined that the H4 weld meets the structural margin requirements for continued operation for at least one additional fuel cycle following RFO6.

2. BACKGROUND AND SUMMARY OF H4 CRACK INDICATIONS

An inspection was performed on the RPV shroud circumferential welds at Limerick Unit 2 during the Spring 1999 RFO5 outage. The inspections consisted of a UT examination of the circumferential welds. During the inspections, indications were found in several circumferential welds. This report addresses the structural evaluation of the H4 weld only. The inspection data for the H4 weld is included in the Appendix A.

Due to the length of the cracking in the H4 weld, a detailed structural evaluation of the weld was performed for one cycle (Ref. 1). In the spring of 2001, NobleChem™ will be implemented following shutdown of the plant. The objective of this report is to update the earlier structural evaluation to include the consideration of operation for an additional cycle after the implementation of NobleChem™. The new analysis considers the reduced crack growth in the H4 weld heat affected zone as a result of NobleChem™ implementation for the additional two years. The report provides the analysis to justify continued operation for two complete fuel cycles since the finding of the indications at H4 during RF05: one fuel cycle (24 months) under normal water chemistry, and one cycle (24 months) under hydrogen water chemistry with NobleChem™.



3. STRUCTURAL MARGIN ASSESSMENT

3.1. ASSUMPTIONS

Several conservative assumptions were made throughout the report. They included the following:

1. A bounding crack growth rate of 5×10^{-5} in/hr will be used for both length and depth for the current cycle (through spring 2001). For the next cycle, a crack growth rate of 1.4×10^{-5} in/hr will be used for depth. The basis for this crack growth rate is detailed in Appendix C.
2. 16,000 hours of operation will be used in the evaluation, based on a 24 month cycle.
3. A UT uncertainty of 0.131 inches will be used for crack depths, which is consistent with BWRVIP-03 (Ref. 2).
4. It is assumed that NobleChem™ will be applied during the spring RF06 outage and during the next cycle, the plant will be operated with 90% HWC availability.
5. All other assumptions are stated in the body of the report.

3.2. STRUCTURAL EVALUATION METHODOLOGY

Section 4.0 of BWRVIP-01 (Ref. 3) describes the flaw evaluation methodology suggested for use in evaluating cracking in core shrouds. Three techniques for the flaw evaluation are recognized: (1) linear elastic fracture mechanics (LEFM), (2) limit load, and (3) elastic-plastic fracture mechanics (EPFM). The LEFM methodology coupled in addition to the limit load approach is appropriate when the fluence level at a weld exceeds 3×10^{20} n/cm² ($E > 1$ MeV). At lower fluence levels, only limit load evaluation is necessary. The EPFM approach may be used in lieu of LEFM when deemed necessary to demonstrate additional margin.



3.3. H4 ANALYSIS

The H4 weld was considered to be in the beltline region (estimated peak fluence greater than 3×10^{20} n/cm²) and therefore, both a limit load and an LEFM evaluation was conducted for this weld. This methodology is consistent with the methodology described in the preceding section. The fluence at the end of cycle 6 is estimated to be 5.8×10^{20} n/cm² and is estimated to be at 7.3×10^{20} n/cm² at the end of cycle 7. (Ref. 4)

Figure 3-1 shows the crack profile of the H4 weld. Approximately 60% of the H4 weld was inspected, and the maximum observed crack depth was 0.11 inches. In fact, of the 36 indications observed at H4, 35 indications had a depth of 0.10 inch or lower. Only one observed indication had a depth of 0.11 in.

Based on the inspection observations, a 360° part through-wall crack was assumed for the LEFM evaluation. The crack depth was assumed to have an initial depth (i.e., before the application of NDE uncertainty and projected crack growth) equal to the maximum indication depth reported at the H4 weld (0.11 in). Thus, the initial crack depth in the clean weld regions as well as the inaccessible weld regions was assumed equal to the maximum measured depth.

The initial assumed 0.11 inch crack depth was increased to account for UT uncertainty (0.131 in) and crack growth (5×10^{-5} in/hr x 16,000 hrs for the current cycle + 1.4×10^{-5} in/hr x 16,000 hrs for the upcoming cycle). The resulting end-of-cycle crack depth was found to be $0.11 + 0.131 + 0.80 + 0.224 = 1.265$ in.

3.3.1. LEFM Analysis

For the LEFM analysis, a fracture mechanics solution for a single edge notch flat plate (Ref. 6) was conservatively applied. This approach is considered conservative since the flat plate solution includes back wall bending caused by the eccentricity of the applied load, which is not present in the cylindrical model. The solution is found by the following formula:

$$K = F * \sigma * \sqrt{(\pi * a)} \quad (4-1)$$



where: K = stress intensity
 F = the geometrical scaling factor
 σ = primary membrane plus primary bending stress, and
 a = crack depth

3.3.2. Limit Load Analysis

Limit load analysis is concerned with gross failure of the shroud. Limit load calculations for the H4 weld were performed using the Distributed Length Ligament computer program (Ref. 5). The flow stress was taken as $3S_m$. The S_m value for the shroud material (Type 304L stainless steel) is 14.4 ksi at the approximate normal operating temperature of 550°F.

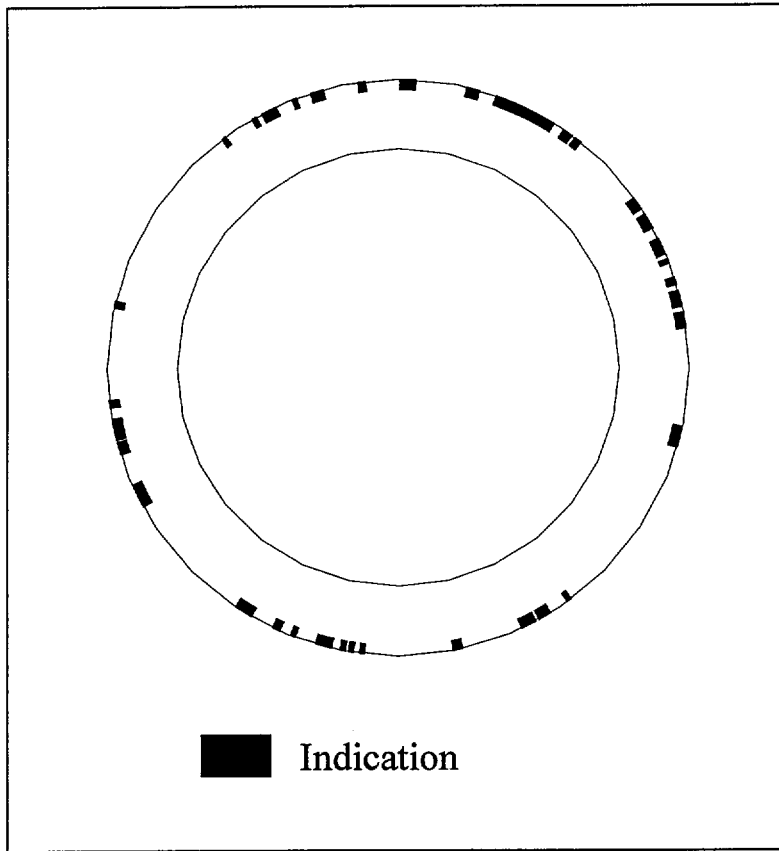


Figure 3-1. H4 Crack Profile



3.4. ANALYSIS RESULTS

The calculated membrane and bending stress magnitudes for the normal/upset and emergency/faulted operating conditions are summarized in Table 3-1. The stresses were calculated based on loads determined in the Reference 7 report. From the calculated stresses, the normal/upset condition was determined to be limiting.

The methodology discussed in the previous section was used to evaluate structural margins at the H4 shroud circumferential weld. Both a limit load and an LEFM evaluation were performed. In each case, an allowable flaw depth was calculated based on a 360° flaw. The allowable flaw depth was then compared to the end-of-cycle crack depth of 1.265 in. As shown in Table 3-2, the end-of-cycle crack depth (1.265 in) is less than the limiting allowable flaw size of 1.66 in. Thus, structural margin exists for the H4 weld.

Table 3-1. Membrane and Bending Stresses for Normal/Upset and Emergency/Faulted Conditions

Weld Location	Pressure Axial Stress (ksi)		Bending Moment Stress (ksi)	
	Upset	Faulted	Upset	Faulted
H4	0.318	0.767	1.154	1.967

**Table 3-2. H4 Results
(Normal & Upset Conditions Were Limiting)**

Weld Location	End of Cycle Crack Depth	LEFM Allowable Crack Depth	Limit Load Allowable Crack Depth
H4	1.265	1.66	1.88



4. CONCLUSIONS

An evaluation of the Limerick Unit 2 shroud H4 weld was performed. Based on the observed cracking during the RFO5 refueling outage, the evaluations assumed a 360° part through-wall crack. An allowable flaw depth was calculated for the H4 weld and compared to the end-of-cycle flaw depth. The evaluation determined that the H4 weld meets the structural margin requirements for continued operation for at least one additional fuel cycle following RFO6, given that NobleChem™ with HWC at 90% availability is maintained after RF06.



5. REFERENCES

1. "The Evaluation of Limerick Unit 2 Shroud Cracking for at Least One Fuel Cycle of Operation", GENE B13-02010-33NP, GE Nuclear Energy, June 1999.
2. BWRVIP-03, "Reactor Pressure Vessel and Internals Examination Guidelines," October 1995.
3. BWRVIP-01, Rev. 2, "BWR Core Shroud Inspection and Flaw Evaluation Guidelines," October 1996.
4. Internal Letter: S. Wang to M.L. Herrera, dated April 10, 1995.
5. BWR Core Shroud Distributed Ligament Length (DLL) Computer Program (Version 2.1), BWRVIP-20, December 1996.
6. Tada, H., Paris, P. and Irwin, G., "The Stress Analysis of Cracks Handbook", Del Research Corp., 1985 Edition.
7. "Core Shroud Loads at Horizontal welds H1 through H8," GENE-B13-02066-00-20-LT1, Revision 0, GE Nuclear Energy, September 19, 2000.



APPENDIX A: UT DATA

(Ref. 1)

Weld H4

Examination of Top Side of Weld - 45° & ODCr Coverage

Total Scan Length Examined (Deg.)	229.65°	Shroud Thickness (in.)	2.00
Total Scan Length Examined (in.)	415.08	Circumference (in.)	650.89
Percent of Weld Length Examined	63.79%	Inches per Degree	1.81
Percent of Examined OD Weld Length Flawed	40.85%	Total Flawed Length (in.)	169.80
Percent of Total OD Weld Length Flawed	26.08%	Total Flawed Length (Deg.)	93.81°

OD 93.81

Weld H4

		45-ODCr										
	Looking Down Data Files	ODCr Scan Start	ODCr Scan End	45° Scan Start	45° Scan End	Scan Length	45-ODCr Coverage	45-ODCr Overlap	Ligament Start	Ligament End	Ligament Length	
TriModal	H4011-1	6.06°	13.76°	5.01°	12.71°	7.70°	8.75°		5.01°	13.76°	8.75°	
TriModal	H4026-1	16.98°	25.78°	15.93°	24.73°	8.80°	9.85°	5.77°	15.93°	25.78°	20.53°	
TriModal	H4026-2	21.08°	35.46°	20.01°	35.41°	15.40°	16.45°					
TriModal	H4056-1	51.06°	66.48°	50.01°	65.41°	15.40°	16.45°	13.03°	50.01°	126.92°	76.91°	
TriModal	H4083-1	54.48°	69.88°	53.43°	68.83°	15.40°	16.45°	1.43°				
TriModal	H4078-1	69.50°	84.90°	68.45°	83.85°	15.40°	16.45°	1.47°				
TriModal	H4098-1	84.48°	99.88°	83.43°	98.83°	15.40°	16.45°	1.45°				
TriModal	H4108-1	99.48°	114.88°	98.43°	113.83°	15.40°	16.45°	4.41°				
TriModal	H4116-1	111.52°	126.92°	110.47°	125.87°	15.40°	16.45°					
Trimodal(SC)	H4168-1	164.72°	170.77°	163.67°	169.72°	6.05°	7.10°		163.67°	170.77°	7.10°	
TriModal	H4191-0	183.63°	194.08°	182.58°	193.03°	10.45°	11.50°	9.07°	182.58°	219.88°	37.30°	
TriModal	H4191-1	186.06°	196.51°	185.01°	195.46°	10.45°	11.50°	4.00°				
TriModal	H4198-1	193.56°	204.01°	192.51°	202.96°	10.45°	11.50°	4.00°				
TriModal	H4206-1	201.06°	211.51°	200.01°	210.46°	10.45°	11.50°	8.08°				
TriModal	H4213-1	204.48°	219.88°	203.43°	218.83°	15.40°	16.45°					
TriModal	H4243-1	235.55°	249.85°	234.50°	248.80°	14.30°	15.35°	1.40°	234.50°	306.48°	71.98°	
TriModal	H4258-1	249.50°	264.90°	248.45°	263.85°	15.40°	16.45°	1.45°				
TriModal	H4273-1	264.50°	279.90°	263.45°	278.85°	15.40°	16.45°	1.45°				
TriModal	H4288-1	279.50°	294.95°	278.45°	293.90°	15.45°	16.50°	4.92°				
TriModal	H4296-1	291.08°	306.48°	290.03°	305.43°	15.40°	16.45°					
Trimodal(SC)	H4341-3	344.72°	350.77°	343.67°	349.72°	6.05°	7.10°		343.67°	350.77°	7.10°	
Total Ligament Length:											229.65°	
Percentage of Total Weld Length:											63.79%	

(SC) = Suction Cup Scanner

REVIEWED PECO NUCLEAR
NDE SERVICES BRANCH *J. J. Hayden* MAY 12 '99

John J. Hayden 5/12/99

05/12/99 WED 17:41 FAX 610 718 3078

PECO/LGS SMB 2FL3

14003

Weld H4

Flaw No.	Weld Side	Initiating Surface	Flaw Start (Degrees)	Flaw End (Degrees)	Flaw Length (Degrees)	Flaw Length (Inches)	Length Search Unit	Maximum Flaw Height	Flaw Thru-Wall Percent	Remaining Ligament (Inches)	Through-Wall Search Unit
1	NS	OD	7.79°	11.09°	3.30°	5.97	ODCr	0.10	5.00%	1.90	45°
2*	NS	OD	12.11°	15.49°	3.38°	6.12	ODCr	0.10	5.00%	1.90	45°
3	NS	OD	16.59°	18.24°	1.65°	2.99	ODCr	0.10	5.00%	1.90	45°
4	NS	OD	21.06°	22.16°	1.10°	1.99	ODCr	0.10	5.00%	1.90	45°
5*	NS	OD	23.03°	26.56°	3.53°	6.39	ODCr	0.10	5.00%	1.90	45°
6	NS	OD	28.78°	32.06°	3.30°	5.97	ODCr	0.10	5.00%	1.90	45°
7	NS	OD	33.18°	35.91°	2.75°	4.98	ODCr	0.10	5.00%	1.90	45°
8	NS	OD	51.13°	52.78°	1.65°	2.99	ODCr	0.10	5.00%	1.90	45°
9	NS	OD	53.33°	55.53°	2.20°	3.98	ODCr	0.10	5.00%	1.90	45°
10*	NS	OD	57.68°	70.68°	12.90°	23.35	ODCr	0.11	5.50%	1.89	45°
11	NS	OD	73.88°	76.63°	2.75°	4.98	ODCr	0.10	5.00%	1.90	45°
12	NS	OD	86.68°	89.98°	3.30°	5.97	ODCr	0.10	5.00%	1.90	45°
13	NS	OD	96.58°	98.23°	1.65°	2.99	ODCr	0.10	5.00%	1.90	45°
14	NS	OD	104.98°	107.73°	2.75°	4.98	ODCr	0.10	5.00%	1.90	45°
15	NS	OD	110.48°	111.58°	1.10°	1.99	ODCr	0.10	5.00%	1.90	45°
16*	NS	OD	114.82°	118.12°	3.30°	5.97	ODCr	0.10	5.00%	1.90	45°
17	NS	OD	119.22°	120.32°	1.10°	1.99	ODCr	0.10	5.00%	1.90	45°
18	NS	OD	126.37°	127.47°	1.10°	1.99	ODCr	0.10	5.00%	1.90	45°
19	NS	OD	166.20°	167.70°	1.60°	2.72	ODCr	0.10	5.00%	1.90	45°
20	NS	OD	186.06°	187.71°	1.65°	2.99	ODCr	0.10	5.00%	1.90	45°
21	NS	OD	189.91°	194.31°	4.40°	7.96	ODCr	0.10	5.00%	1.90	45°
22	NS	OD	194.66°	197.41°	2.75°	4.98	ODCr	0.10	5.00%	1.90	45°
23	NS	OD	203.81°	208.76°	4.95°	8.96	ODCr	0.10	5.00%	1.90	45°
24	NS	OD	236.84°	239.69°	2.75°	4.98	ODCr	0.10	5.00%	1.90	45°
25	NS	OD	244.35°	246.00°	1.65°	2.99	ODCr	0.10	5.00%	1.90	45°
26	NS	OD	248.20°	249.30°	1.10°	1.99	ODCr	0.10	5.00%	1.90	45°
27	NS	OD	253.40°	256.70°	3.30°	5.97	ODCr	0.10	5.00%	1.90	45°
28	NS	OD	258.35°	259.45°	1.10°	1.99	ODCr	0.10	5.00%	1.90	45°
29	NS	OD	260.00°	261.10°	1.10°	1.99	ODCr	0.10	5.00%	1.90	45°
30	NS	OD	262.20°	263.30°	1.10°	1.99	ODCr	0.10	5.00%	1.90	45°
31	NS	OD	280.70°	282.70°	2.00°	3.62	ODCr	0.10	5.00%	1.90	45°
32	NS	OD	294.93°	298.23°	3.30°	5.97	ODCr	0.10	5.00%	1.90	45°
33	NS	OD	298.78°	301.53°	2.75°	4.98	ODCr	0.10	5.00%	1.90	45°
34	NS	OD	305.38°	306.48°	1.10°	1.99	ODCr	0.10	5.00%	1.90	45°
35	NS	OD	343.70°	344.70°	1.00°	1.81	ODCr	0.10	5.00%	1.90	45°
36	NS	OD	344.70°	348.20°	3.50°	6.34	ODCr	0.10	5.00%	1.90	45°
					93.81°	169.80					

REVIEWED PECO NUCLEAR NDE SERVICES BRANCH *ll. b. b.* MAY 12 '99

John J. Hayden 5/12/99



GENE B13-02080-00-03NP

***APPENDIX B: The Beneficial Effect of Reduced Corrosion Potential on
the Stress Corrosion Crack Growth Rates of Irradiated Stainless Steel***

***APPENDIX B: The Beneficial Effect of Reduced Corrosion Potential on
the Stress Corrosion Crack Growth Rates of Irradiated Stainless Steel***

August 2000

Dr. Peter L. Andresen,
Physical Metallurgy Laboratory
GE Corporate R&D Center
P.O. Box 8, K1-3A39
Schenectady, NY 12301

APPENDIX B: *The Beneficial Effect of Reduced Corrosion Potential of the Stress Corrosion Crack Growth Rates of Irradiated Stainless Steel*

1. Introduction

This document provides a brief overview of IASCC, then summarizes the evidence to support the very beneficial effect of corrosion potential on stress corrosion crack (SCC) growth rates on neutron irradiated stainless steels. To present the compelling case that exists, this review focuses on following related areas of evidence with the underlying theme that there is a strong commonality among all “types” of SCC in structural materials in high temperature water, including the most relevant category – IGSCC in austenitic stainless steels.

- I.** Common characteristics and water chemistry dependencies of unirradiated and irradiated stainless steel
- II.** Effects of corrosion potential on SCC of unirradiated materials in unirradiated environments
- III.** Effects of corrosion potential on SCC of unirradiated materials in irradiated environments
- IV.** Effects of corrosion potential on SCC of neutron irradiated materials in the laboratory
- V.** Effects of corrosion potential on SCC of neutron irradiated materials under irradiated conditions in test reactors and BWRs
- VI.** Benefit of NobleChem™ under all conditions

This review presents some specific proprietary crack growth rate data, much of it unique to GE, to support the factor of improvement that has been discussed for the NobleChem™ in conjunction with Hydrogen Water Chemistry. These data include tests performed on highly irradiated materials as well as cold worked L-grade type 304 stainless steels. The report also briefly discusses the predicted factors of improvement made using the GE Irradiated PLEDGE code which confirms the benefit. Finally, a specific crack growth rate is recommended for use in the structural analysis described in the body of the report.

2. Overview of Irradiation Assisted Stress Corrosion Cracking in Stainless Steels

Irradiation assisted stress corrosion cracking (IASCC) is the sub-critical cracking of materials exposed to ionizing irradiation [1-8], although it sometimes viewed more restrictively to represent environmentally assisted cracking of irradiated materials (not unirradiated materials exposed to radiolytic environments). IASCC is most often associated with light water reactor (LWR) environments involving high temperature water and neutron irradiation exposure, which alters many material properties and causes radiolysis of water. While initially viewed as a unique and hopelessly complex form of cracking, IASCC is now broadly interpreted as a radiation accelerated process within the spectrum of environmental cracking (Figure 1).

The dependence of IASCC on neutron fluence for austenitic stainless steel is shown in Figure 2 for BWR control blade sheaths [9,10],

Above a fluence of $\approx 2 \times 10^{20}$ n/cm² (energy >1 MeV), which corresponds to nearly ≈ 0.3 lattice displacements per atom (dpa), an increase in intergranular cracking is observed. This "threshold" fluence must be viewed as a pragmatic limit since IGSCC occurs at zero fluence in unirradiated, unsensitized stainless steels in ultra high purity water, even in even H₂ deaerated high purity water [12,13] (Figure 5).

Among the various factors that alter IGSCC (and IASCC) susceptibility, corrosion potential is among the most potent and most important, because it can be controlled in existing plants.

IASCC has been extensively observed, despite the use, e.g., of solution annealed materials and low design stresses. As summarized in references [1-9], initial reports of IASCC occurred in the early 1960s in fuel elements, where high stresses associated with fuel swelling were considered an essential and unusual ingredient. However, IASCC was subsequently reported in a variety of high and low stress core components and in-situ test specimens in boiling water reactors (BWR), commercial pressurized water reactors (PWR), US Navy test PWRs, and steam generating heavy water reactors (SGHWR). Evaluation of IGSCC in cold worked, irradiated stainless steel baffle bolts in PWRs has shown that low corrosion potential does not provide immunity to IASCC, although the higher temperature in PWRs can significantly increase SCC susceptibility. IASCC concerns also exist in applications such as high level radioactive waste containers and fusion reactors. In all cases, IASCC poses special concerns related to difficulties in

inspection, and repair or replacement. In 1986 an International Cooperative Group on IASCC was formed [] with the primary objective of developing fundamental understanding and life prediction capability for IASCC, which is crucial to LWR plant management and life extension.

2.1. Major Findings of the Last Fifteen Years of IASCC Research

Based on both laboratory and field experience, the critical findings of the last 15 years of research into IASCC include:

1. There is inherent SCC susceptibility in high temperature water of all structural materials and alloy types under almost all conditions, although very dramatic differences in kinetics also occur.
2. Major contributing factors to SCC susceptibility include neutron fluence, cold work, corrosion potential, water purity, temperature, and loading.
3. The interactive nature of the influential parameters makes their individual contribution to SCC appear complex, and changes the apparent threshold in any one parameter. This, coupled with the obvious importance of (test/exposure) time on the appearance of IASCC makes any "threshold" uncertain and even of dubious significance. A reasonable "working threshold" fluence of about 2×10^{20} n/cm² can be used for annealed components in high purity oxidizing environments, but some radiation enhancement (esp. in sensitized stainless steels) can be expected at lower fluences. Conversely, under low potential conditions (e.g., BWR NobleChem™ or PWR), the kinetics of SCC are dramatically reduced and the "working threshold" is $\approx 3 \times 10^{21}$ n/cm² at 288°C ($\approx 10^{21}$ n/cm² at 325 °C), as discussed in later sections.
4. The state of quality and reproducibility of most IASCC (indeed, all SCC) measurements is not consistently high, and data must be carefully compared and verified against other observations. The origins of these problems include the complexity of the experiments and number of disciplines that must be mastered, as well as to the nature of SCC.
5. Radiation promotes SCC via several phenomena:
 - Radiolysis can produce an oxidizing environment that increases the corrosion potential (this is suppressed by the high H₂ fugacity in PWRs)
 - Radiation induced segregation (RIS, or RS) produces compositional differences very near to grain boundaries (). While into the mid-1990s there was a heavy preoccupation with the possible effects of impurities like P, S, Si, N, and B, there is now a broader acceptance of the primary importance of Cr depletion. Cr depletion is most important in oxidizing environments (that produce a pH-shifted crevice and crack chemistry); in low potential BWR and PWR environments, its role is secondary.
 - Radiation hardening (RH) causes dramatic increases in yield strength by generating point defect damage and small diameter vacancy and interstitial

loops. These are very strong barriers to initial dislocation motion, but once a few dislocations move along a slip plane, they clear the point defects and most of these very fine obstacles. This creates a "dislocation channel" of softened material in which subsequent dislocation motion readily occurs. Thus, in almost all cases, highly irradiated materials are not brittle, but highly ductile on a local scale. This also results in strain softening (not strain hardening), and necking often develops at low strains, leading to low uniform elongation but high reduction in area near the fracture. Because strain softening occurs, ASTM fracture mechanics K /size criteria [14] must be interpreted and applied with caution. It is believed that radiation hardening acts in a similar fashion to cold work, as both processes increase the yield strength and enhance SCC growth rates at high and low corrosion potential [1-3,12,13].

- Radiation creep / relaxation is a relatively well behaved, consistent process that tends to enhance SCC by promoting dislocation motion. Under constant displacement conditions (e.g., for weld residual stresses or baffle bolts), radiation creep produces substantial stress relaxation within a few dpa, which is an important factor in understanding and predicting the behavior of such components.

3. The Beneficial Effect of Reduced Corrosion Potential of the Stress Corrosion Crack Growth Rates of Irradiated Stainless Steel

3.1. *Common characteristics and water chemistry dependencies of unirradiated and irradiated stainless steel*

Early investigators suggested that IASCC was a unique phenomenon, largely because of its supposedly unusual characteristics (e.g., its occurrence in solution annealed stainless steel) and the myriad of hypothetical radiation effects on cracking. However, as new data have been generated and critical experiments performed, the basis for viewing IASCC as radiation-enhanced form of environmental cracking have become increasing compelling, including:

- The observation of similar dependencies among cracking of unirradiated materials in the laboratory, and irradiated materials in the laboratory, test reactor, and in-plant
- The recognition that radiation segregation produces significant chromium depletion near grain boundaries in initially solution annealed materials. These chromium profiles are broadly characteristic of thermal sensitization (), although they are much narrower and generally not as deep. The similarity in SCC response was demonstrated by comparing normal thermal sensitization

profiles with narrow profiles

- The observation that increasing yield strength by cold work enhances SCC growth rates in both aerated and deaerated (pure) water, in the absence or presence of sensitization. This is a strong parallel to the response of irradiated stainless steels, which show increased crack growth rates with fluence. In deaerated water, there should be little effect of sensitization, so the enhancement in growth rate is primarily attributable to the increase in yield strength from irradiation.

- The observation that little or no intergranular cracking occurs in inert environments under similar temperature and loading conditions. Also, cracks are generally observed to initiate from the water side of components.

Both phenomenological interpretation and predictive modeling relies on this evidence in support of a “radiation-enhanced” view of IASCC as a basis to extend our existing understanding and predictive modeling for unirradiated stainless steels to include irradiated effects.

3.2. *Effects of corrosion potential on SCC of unirradiated materials in unirradiated environments*

There are large number of observations that demonstrate the importance of corrosion potential on SCC of unirradiated materials in unirradiated environments. In addition to extensive slow strain rate testing, more carefully controlled and quantitative fracture mechanics crack growth rate studies show that corrosion potential is the strongest factor in controlling SCC kinetics.

Precise crack growth rates at low potential are difficult to measure because the rates are so low. However, there is no question that the rates are indeed low at low corrosion potential

An additional factor in having confidence that corrosion potential will reduce SCC growth rates relates to the issue of achieving a consistently low potential throughout the relevant regions of a BWR. With hydrogen water chemistry, this is a valid concern for the in-core regions of all plants and, in some less responsive plants, even in the recirculation piping and bottom head. However, by making the surfaces catalytic using NobleChem™, this concern is eliminated, at least in areas where stoichiometric excess molar ratio of H₂ to O₂ can be maintained (exceptions occur primarily in areas where the steam fraction (or “quality”) is high, e.g., at the core spray piping). It has been clearly shown that NobleChem™ works even at very high oxidant levels – both on corrosion potential (Figure 17) and SCC (Figure 18) – and that the surface coverage necessary to achieve these benefits is very low, both at low flow rate and high flow rate (Figure 18).

3.3. *Effects of corrosion potential on SCC of unirradiated materials in irradiated environments*

As we consider irradiated water chemistry or irradiated materials, the experience base decreases.

The results of these experiments establish that the oxidizing radiolytic conditions do promote crack growth. However, the environments are not fundamentally different than those produced in the laboratory using high oxygen levels, 2000 to 8000 ppb. The measured enhancements in corrosion potential also substantiate this.

3.4. *Effects of corrosion potential on SCC of neutron irradiated materials in the laboratory*

There has been a moderate number of laboratory studies performed on BWR neutron irradiated stainless steels, where the vast majority have been done using the slow strain rate technique. The strong effect of corrosion potential was demonstrated nearly twenty years ago

**3.5. *Effects of corrosion potential on SCC of neutron irradiated materials
under irradiated conditions in test reactors and BWRs***

4. **Summary and Conclusions: Benefit of Reduced Corrosion Potential on Irradiated Crack Growth Rates**

Very compelling evidence exists that stress corrosion crack growth rates of all BWR structural materials, unirradiated or irradiated, are very strongly affected by corrosion potential. Additional testing under specific, relevant and well-controlled conditions is recommended to more precisely quantify the factor of improvement under irradiated conditions, but a benefit of changing to low potential conditions can be conservatively stated as an order of magnitude reduction in crack growth rate.

Without NobleChem™, it is difficult to be assured that low potential conditions are met in the locations of interest in a BWR. With NobleChem™ and stoichiometric excess H₂, there is ample evidence that low potential conditions are met in the relevant locations (low potential is not achieved in regions where the steam quality is high, e.g., where the fuel channel and bypass water mix above the core).

It must be recognized that the benefit is not realized when stoichiometric H₂ does not exist (e.g., H₂ injection is stopped), or the water purity becomes very poor. In good purity water (<0.3 μS/cm), the change to low potential produces a very rapid reduction in growth rate (almost always much faster reduction than the subsequent increase in crack growth rate when the potential is increased), so that a linear attribution of "H₂ on" and "H₂ off" periods is appropriate. If the water purity is very poor, this rough symmetry when changing between high and low corrosion potential no longer holds, although such occasions are so rare in modern BWR operation as to be nearly irrelevant. Note also that under low corrosion potential operation there is a very large tolerance for increases in solution conductivity

5. References

1. P.L. Andresen, "Irradiation Assisted Stress Corrosion Cracking", in Stress Corrosion Cracking: Materials Performance and Evaluation, Ed. R.H. Jones, ASM, Materials Park, 1992, p.181-210.
2. P.L. Andresen, F.P. Ford, S.M. Murphy & J.M. Perks, "State of Knowledge of Radiation Effects on Environmental Cracking in Light Water Reactor Core Materials", Proc. 4th Int. Conf. on Environmental Degradation of Materials in Nuclear Power Systems - Water Reactors, NACE, p.1-83 to 1-121, 1990.
3. F.P. Ford, P.L. Andresen & A.J. Jacobs, "Life Prediction of Irradiated Components Subject to Environmentally Assisted Cracking", Int. Symp. On Plant Aging & Life Prediction of Corrodible Structures Sapporo, Japan, May 15-18, 1995.
5. G.S. Was & P.L. Andresen, "Irradiation Assisted Stress Corrosion Cracking in Austenitic Alloys", Journal of Metals, Vol. 44, No. 2, p. 8-13, April 1992.
6. A.J. Jacobs & G.P. Wozadlo, "Irradiation Assisted Stress Corrosion Cracking As a Factor in Nuclear Power Plant Aging", Proc. Int. Conf. on Nuclear Power Plant Aging, Availability Factor and Reliability Analysis, San Diego, CA, ASM, p.173, 1985.
7. F. Garzarolli, H. Rubel & E. Steinberg, "Behavior of Water Reactor Core Materials with Respect to Corrosion Attack", Proc. First Int. Symp. on Environmental Degradation of Materials in Nuclear Power Systems - Water Reactors, NACE, 1984, p.1-24.
8. H. Hanninen & I. Aho-Mantila, "Environment-Sensitive Cracking of Reactor Internals", Proc. Third Int. Symp. on Environmental Degradation of Materials in Nuclear Power Systems - Water Reactors, AIME, 1987, p.77-92.
9. G.M. Gordon & K.S. Brown, "Dependence of Creviced BWR Component IGSCC Behavior on Coolant Chemistry", Proc. 4th Int. Conf. on Environmental Degradation of Materials in Nuclear Power Systems - Water Reactors, NACE, p.14-46 to 14-62, 1990.
10. K.S. Brown & G.M. Gordon, "Effects of BWR Coolant Chemistry on the Propensity for IGSCC Initiation and Growth in Creviced Reactor Internals Components", Proc. Environmental Degradation of Materials in Nuclear Power Systems - Water Reactors, AIME, p.243-248, 1987.
12. T.M. Angeliu, P.L. Andresen, J.A. Sutliff and R.M. Horn, "Intergranular Stress Corrosion Cracking of Unsensitized Stainless Steels in BWR Environments", Proc. Ninth Int. Symp. on Environmental Degradation of Materials in Nuclear Power Systems - Water Reactors, AIME, 1999.
13. P.L. Andresen, T.M. Angeliu, W.R. Catlin, L.M. Young and R.M. Horn, "Effect of Deformation on SCC of Unsensitized Stainless Steel", Corrosion/2000, Paper 00203, NACE, 2000.

14. "Standard Test Method for Plane Strain Fracture Toughness of Metallic Materials", E399-90 (re-approved 1997), 1997 Annual Book of ASTM Standards, Volume 03.01, ASTM, 1997. Also, "Standard Test Method for Constant Load Amplitude Fatigue Crack Growth Rates Above 10^{-8} m/cycle", E647-95a, 1997 Annual Book of ASTM Standards, Volume 03.01, ASTM, 1997. Other ASTM standards also apply.

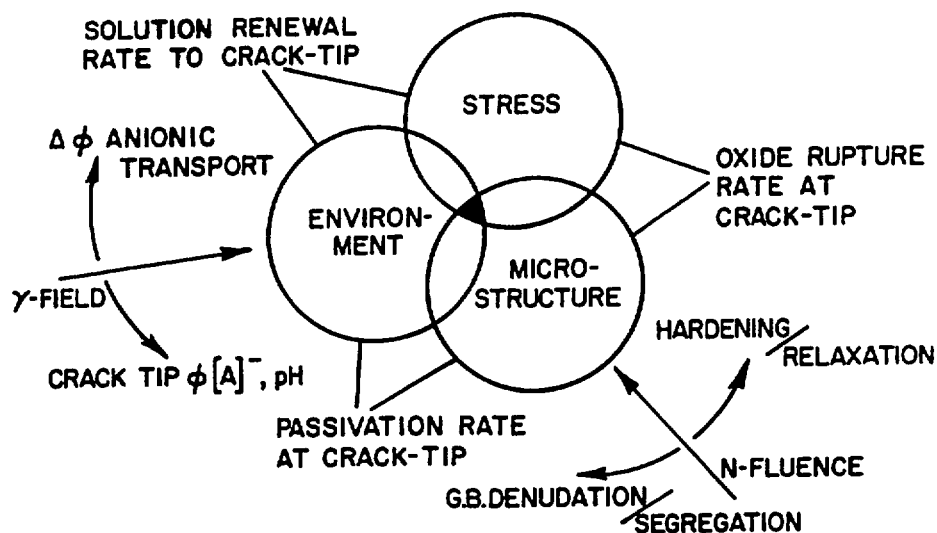
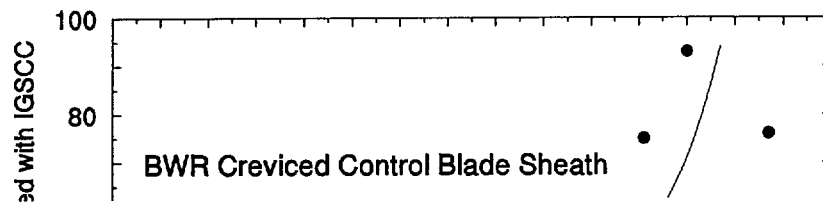


Figure 1. Illustration of engineering factors (stress, environment, and microstructure), underlying fundamental phenomena (mass transport, oxide rupture, and repassivation), and primary effects of radiation on crack advance processes. While initially viewed as a unique and hopelessly complex form of cracking, IASCC is now broadly interpreted as a radiation accelerated process within the spectrum of environmental cracking [1-3].



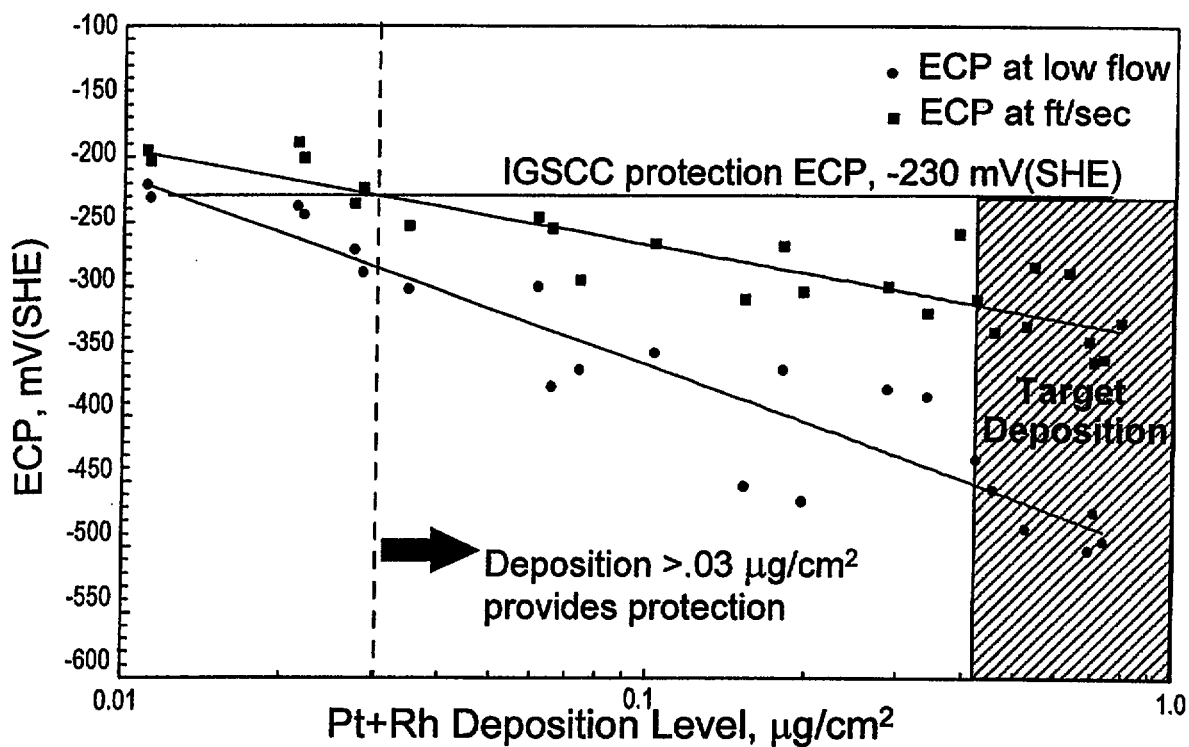
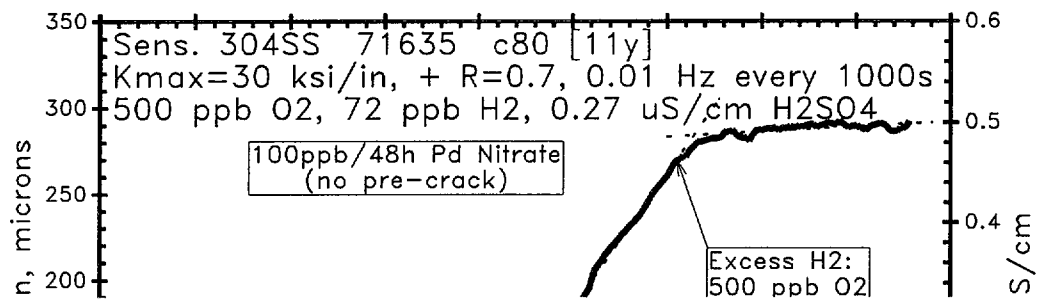


Figure 17. Corrosion potential vs. surface loading of Pt and Rh following NobleChem® treatment showing that very load loadings are adequate to achieve $-0.23 V_{\text{she}}$. Data were obtained in 288 °C pure water containing stoichiometric excess H_2 under low flow and high flow rate conditions [32].







***APPENDIX C: Crack Growth Rates in the High Fluence H4 Shroud
Weld During Operation With NobleChemTM And Hydrogen Water
Chemistry***



Crack Growth Rates in the High Fluence H4 Shroud Weld During Operation With NobleChem™ And Hydrogen Water Chemistry

1. Introduction

Appendix B discusses the benefits of NobleChem™ in reducing crack growth rates for stainless steels in both the un-irradiated and irradiated condition. The Appendix discusses the understanding of SCC process and presents a large body of information on the impact of irradiation on the environment as well as the material itself. The data clearly substantiates that reduction of the corrosion potential through hydrogen injection in conjunction with NobleChem™ significantly reduces crack growth rates in both un-irradiated and irradiated stainless steel materials. The SCC process in irradiated materials is controlled by the same factors as that in conventional IGSCC of sensitized stainless steel. Thus, the corrosion potential of the environment is a key parameter in determining the rate of crack growth. The purpose of this Appendix is to quantify the amount of reduction that is imparted by this change in the corrosion potential, ECP. This quantification will be done in two ways. First, the available laboratory crack growth rate data discussed in Appendix B will be used as a basis for specific factors of improvement. Secondly, this Appendix will briefly describe and use the GE Irradiated PLEDGE model to also assess the expected factor of improvement attributable to the change from normal water chemistry (NWC) to hydrogen water chemistry (HWC). The model includes several important parameters in addition to the water chemistry parameters. It includes the effect of material changes with irradiation that enhance crack growth rates and includes the overall impact of the irradiation environment on crack growth rates. It also includes consideration of residual stress relaxation which lowers the stresses driving crack growth.

Using these factors of improvement from the data and from the modeling assessments as a basis, the crack growth rate to be used in the Limerick Unit 2 H4 evaluation will be defined. This section will include a discussion of the impact of HWC availability, the time on and off HWC, on the average growth rate for the cycle.

2. Factors of Improvement Observed in Laboratory Crack Growth Tests on Irradiated Materials

As discussed and presented in Appendix B, there have only been a few different fracture mechanics crack growth studies that have been performed.



This is needed to determine the crack growth rate for use in the upcoming cycle at the Limerick Unit 2. Figures 1 through 3 (taken from Appendix B) display key plots of some of these special tests. Review of the appropriate test periods allows a factor of improvement to be determined.

the factor of improvements were found to be 8.5 to 35 for the CT specimen and greater than 100 for the bend specimen. the factor of improvements were found to be 19, 77 and 12.5 based on the rates with and without HWC. While these tests were difficult to perform, these results certainly do support the important role of ECP on crack growth in irradiated materials and establish that the rates are reduced by a factor of greater than 10 in HWC.

3. Overview of the GE Irradiated PLEDGE Model

Using the principles of stress corrosion cracking, the PLEDGE model was developed by GE CR&D over 15 years ago to predict crack growth rates for sensitized stainless steel. This was later extended to irradiated stainless steel. It can be used to predict crack growth rates in different austenitic stainless steel structural components including core internal welded structures [1-3]. Since it is built on the fundamentals of stress corrosion cracking, it can also be used to predict the beneficial effects of low corrosion potential for both unirradiated and irradiated stainless steels.

The GE PLEDGE model is based on the slip-dissolution film-rupture SCC process. The crack propagation rate, V_t is defined as a function of two constants, A and n, and the crack tip strain rate, $\dot{\epsilon}_{ct}$. The values of the constants are dependent on the material condition (Electrochemical Potentiokinematic Reactivation or EPR value) and the environment (water conductivity and electrochemical corrosion potential or ECP) conditions. Constants A and n are related as follows:

$$V = A (\dot{\epsilon}_{ct})^n \tag{1}$$

where

The crack tip strain rate, $\dot{\epsilon}_{ct}$, is formulated in terms of stress, loading frequency, etc. and is obtained as follows:



$$d\varepsilon_{ct}/dt = CK^4 \quad (2)$$

Where K is the stress intensity factor, a fracture mechanics parameter and $d\varepsilon_{ct}/dt$ is the crack tip strain rate and C is constant that considers the interaction between the gamma field and the fundamental parameters which affect intergranular stress corrosion cracking (IGSCC) of Type 304 stainless steel in a radiation field.

The increase in material sensitization (i.e., EPR) and the changes in the value of constant C as a function of neutron fluence (>1 MeV) is given as the following:

(3)

The parameters input into the GE model to make the crack growth calculation are: stress distribution or stress intensity factor K, initial EPR, fluence or flux, the effect of fluence in relaxing the residual stresses, water conductivity, and ECP.

The stress state relevant to IGSCC growth in a core shroud is a function of the steady state applied stress and the weld residual stresses. The steady applied stress on the shroud is due to core differential pressure and its magnitude is small. The weld residual stresses in cylinder to cylinder welds, representative of the H4 weld, transition from tension to compression in magnitude through the thickness resulting in low stress intensity magnitude in the center of the core shroud thickness [4]. The resultant value of the stress intensity factor (K) for the majority of the depth is less than 15 ksi $\sqrt{\text{in}}$. In addition, the weld residual stress magnitude is actually expected to decrease as a result of relaxation produced by irradiation-induced creep.

The third parameter used in the GE predictive model is the water conductivity. A water conductivity of 0.1 $\mu\text{S}/\text{cm}$ represents the current conductivity of most plants, including Limerick Unit 2.



The lower value would be appropriate for factor of improvement assessments and the higher value for a crack growth rate calculation. For NobleChem™ with hydrogen water chemistry, the ECP value is always expected to be well below the $-230 \text{ mV}_{\text{she}}$ needed to impart mitigation. Therefore, a value of $-230 \text{ mV}_{\text{she}}$ is a good conservative value to evaluate a factor of reduction in the crack growth rate.

4. Validation of the Beneficial Effects of low corrosion potential using the Irradiated PLEDGE Model

The PLEDGE model is unique in that it is both based on fundamental principles and it has been benchmarked using both un-irradiated and irradiated crack growth rate data including the data discussed earlier. Because of its ability to use material and environmental information, the model is well suited to predicting the decrease in crack growth rate at the H4 core shroud weld location attributable to the implementation of NobleChem and HWC. Therefore, the model has the ability to evaluate the “factor of improvement” as a function of the water chemistry parameters (corrosion potential and conductivity) that are appropriate for a plant (1) operating with HWC following NobleChem™ and (2) adhering to the EPRI Water Chemistry Guidelines (maintaining conductivity below action Level 1). Equally important, it can include the effects of residual stress relaxation in the calculation of crack growth rate. The impact of the stress relaxation is displayed in Figure 4. Using these stress intensity values, Figure 5 displays the expected upper bound crack growth rate for NWC as a function of fluence.

Figure 5 also shows these HWC rates, allowing a comparison for the two water chemistry conditions. The rates are 40 times lower in the NobleChem™-HWC environments with a nominal conductivity of $0.1 \mu\text{S}/\text{cm}$. The ratio of the two rates compares very well with the lab data shown in Figures 1 through 3 and with the understanding of SCC thoroughly documented in Appendix B.

The Irradiated PLEDGE model can also be used to perform FOI calculations at fixed K and conductivity conditions. Table 1 lists the calculated crack growth rates as well as the FOI. It is clear that over the entire range of fluence for the nominal conductivity level, there is a large positive effect of the NobleChem™ environment on reducing crack growth rates. Figure 6 shows these same FOIs graphically for this $0.1 \mu\text{S}/\text{cm}$ conductivity level that represents the Limerick Unit 2 plant conditions.



This model output is consistent with all of the information in Appendix B in predicting the large benefit of the improved HWC/NobleChem™ environment. Overall, the factor of improvement is well in excess of 10. The FOI, calculated over a range of fluence, is also independent of fluence. Applying this assessment to the NRC approved NWC crack growth rate of 5×10^{-5} in/hr for irradiated material, the crack growth rate for the H4 in the presence of NobleChem™ can be at least as low as 0.5×10^{-5} in/hr.

5. Crack Growth Rate for H4 during Operation with NobleChem™ and HWC

The current accepted through-wall crack growth rate for reactor core internals has been defined to be 2.2×10^{-5} in/hr for fluences up to 5×10^{20} n/cm². In addition, the NRC has allowed the use of 5×10^{-5} in/hr for fluences greater than 5×10^{20} n/cm² in earlier justifications for continued operation consistent with BWRVIP-01 evaluations

The information given in this Appendix clearly establishes the definite, large benefit of NobleChem with HWC in mitigating SCC processes, including IASCC (which is just an extension of IGSCC as detailed in Appendix B). This produces a significant reduction in the crack growth rate. This “factor of improvement”, provides the basis for a lower crack growth rate for the H4 weld to be used in the upcoming cycle. Even though a lower crack growth rate can be justified, the use of a conservative crack growth rate of rate of 1×10^{-5} in/hr is recommended. This represents a factor of improvement of 5 over that used for the Normal Water Chemistry environment. It should be noted that during periods when HWC is not in effect, the rate to be used is 5×10^{-5} in/hr. With the large amount of industry experience and Limerick Unit 2 being operated on low level HWC, an availability of 90% should easily be achieved during the upcoming cycle. The HWC availability and the proposed growth rate for HWC support the use of an average rate for the cycle of 1.4×10^{-5} in/hr. This average rate is the rate that is used in the H4 evaluation for the upcoming cycle.



6. References

1. Ford, F.P. and Andresen, P.L., "Prediction of Environmentally Assisted Cracking in Boiling Water Reactors, Part I: Unirradiated Stainless Steel Components," GE NEDC-32613, June 1996.
2. Andresen, P.L. and Ford, F. P., "Modeling of Irradiation Effects on Stress Corrosion Cracking Growth Rates," paper 497 presented at Corrosion 89, NACE, New Orleans, LA, April 1989.
3. Andresen, P.L. and Ford, F. P., "Irradiation Assisted Stress Corrosion Cracking: From Modeling and Prediction of Laboratory and In-core Response to Component Life Prediction," paper 419 presented at Corrosion 95, NACE, Orlando, FL, March 1995.
4. "BWR Vessel and Internals Project, Evaluation of Crack Growth BWR Stainless Steel RPV Internals (BWRVIP-14)," EPRI TR- 105873, March 1996.
5. "Design Criteria for Irradiated Stainless Steel in BWR Applications," GENE NEDE-20364, June 1974.
6. "BWR Vessel and Internals Project, BWR Core Shroud Inspection and Flaw Evaluation Guidelines, Revision 2 (BWRVIP-01)," EPRI Report TR-107079, October 1996.



GE Proprietary Information

GENE B13-02080-00-03NP

GENE B13-02080-00-03NP